Journal of Educational Technology and Learning Creativity
Vol. 4, No. 1, June 2026, pp. 321~339
ISSN: 3021-7865, DOI: 10.37251/jetlc.v4i1.3179

Technical Computational Approach for Drug Discovery: in silico Analysis of Non-Edible Parts of *Durio oxleyanus* from Sabah as Enzyme Inhibitors in Diabetes Management

Qomariah Hasanah[1,2], Monica Suleiman[1], Ayu Indayanti Ismail[5], Elfira Jumrah[6], Nur Hasanah[7], Syahriel bin Abdullah[1,3,4]

[1]Institute for Tropical Biology and Conservation, Universiti Malaysia Sabah, Kota Kinabalu, Malaysia
[2]Tadris IPA, Fakultas Tarbiyah dan Tadris, Universitas Islam Negeri Fatmawati Sukarno, Bengkulu, Indonesia
[3]Borneo Research on Algesia, Inflammation and Neurodegeneration (BRAIN) Group, Faculty of Medicine and Health Sciences, Universiti Malaysia Sabah, Kota Kinabalu, Malaysia
[4]Borneo Innovative Centre for Utilization of Resources in Ethnopharmacology (BioCURE), Universiti Malaysia Sabah, Kota Kinabalu, Malaysia
[5]Biotechnology Study Program, Faculty of Mathematics and Natural Sciences, Universitas Sulawesi Barat, Sulawesi Barat Indonesia
[6]Chemistry Department, Faculty Mathematich and Science, Universitas Negeri Makassar, Makassar, Indoensia
[7]Department of Pharmacy, Widya Dharma Husada Tangerang School of Health Science, Banten, Indonesia

Article Info

Article history:

Received Mar 3, 2026
Revised Apr 17, 2026
Accepted May 30, 2026
Online First Jun 15, 2026

Keywords:

Computational
Diabetes
Durio Oxleyanus
Enzyme
Technical

ABSTRACT

Purpose of the study: One strategy for controlling blood glucose levels is to inhibit carbohydrate digestion enzymes, namely α-glucosidase and α-amylase. This study uses a technical computational approach to explore the bioactive potential of the inedible part (husk) of Durio oxleyanus from Sabah as an inhibitor of both enzymes.

Methodology: Hydroalcoholic extracts were analyzed using LC-MS, which identified phenolic and flavonoid compounds including catechin, rutin, quercetin, malvidin-3-O-glucoside, and lucidenic acid D1. Molecular docking simulations were performed against α-glucosidase (PDB ID: 2QMJ) and α-amylase (PDB ID: 1B2Y) using PyRx integrated with AutoDock and AutoDock Vina.

Main Findings: The results showed that several compounds had high binding affinity (ΔG ≤ -7.0 kcal/mol) and interacted stably with polar, aromatic, and hydrophobic residues in the enzyme's active site. Lucidenic acid D1, rutin, catechin, and quercetin-3-O-glucosidase stood out as the main candidates with the lowest binding energy and multipoint interactions that support the formation of stable complexes.

Novelty/Originality of this study: This study has demonstrated significant innovation by revealing the potential of the inedible parts of *Durio oxleyanus* as a source of candidate antidiabetic drugs through a computational approach. The integration of LC-MS profiling and molecular docking enables the efficient identification of bioactive compounds while accelerating the drug discovery process without relying entirely on experimental methods. This research lies in its contribution to the concept of sustainable bioprospecting, the exploration of under-researched local biodiversity, and the multi-target validation of key diabetes enzymes.

Corresponding Author:
Syahriel bin Abdullah,
Institute for Tropical Biology and Conservation, Universiti Malaysia Sabah,
Jalan UMS, 88400, Kota Kinabalu, Malaysia

Email: asyahriel@ums.edu.my

1. INTRODUCTION

Diabetes has now become one of the 21st century's most significant global health issues, with the number of people affected continuing to rise due to lifestyle changes, high-calorie diets, obesity, and an aging population. This condition not only places a burden on the healthcare system but also significantly reduces people's quality of life and productivity [1]-[3]. Diabetes is a serious chronic disease that occurs when the body is unable to produce sufficient insulin or cannot effectively utilize the insulin that is available [4]-[6]. Insulin itself is an important hormone produced by the pancreas that regulates blood sugar levels. If insulin production or function is disrupted, glucose will remain in the bloodstream because it cannot enter the cells, causing hyperglycemia [7]-[9]. Uncontrolled hyperglycemia can trigger various complications, including heart disease, kidney failure, nerve damage, vision problems, and even premature death.

One of the main mechanisms of diabetes is through enzymes that work in the carbohydrate digestive system, namely α-amylase and α-glucosidase enzymes. Alpha-amylase is the main enzyme in the human digestive system, which hydrolyzes starch and converts glycogen into oligosaccharides such as maltose, maltotriose, and oligo glucan [10]-[12]. Alpha-glucosidase, found in the small intestine, breaks down disaccharides (breaking the α-(1→4) glycosidic bond) and then absorbs them. Rapid breakdown of dietary starch causes a postprandial blood sugar spike [13]. Blocking α-amylase and α-glucosidase is one treatment for postprandial hyperglycemia. Currently, diabetes therapy still focuses on pharmacological approaches, such as the use of exogenous insulin, metformin, sulfonylureas, DPP-4 inhibitors, and SGLT2 inhibitors [14], [15]. This treatment is based on the metabolic evaluation of patients with diabetes mellitus using chemical drugs [16]-[18]. Synthetic drugs such as acarbose and miglitol, which inhibit α-amylase and α-glucosidase, can cause stomach upset, vomiting, and diarrhea.

However, the use of chemical drugs often causes long-term side effects, high costs, prolonged dependence, and an impact that is not environmentally friendly [19]. Therefore, alternative therapies are needed that can reduce these risks. One option is the use of natural ingredients. Phytochemical compounds or secondary metabolites in natural ingredients are known to have potential as antidiabetic and antioxidant agents. Various types of natural bioactive compounds such as tannins, flavonoids, catechins, and gallic acid have been identified as having antioxidant properties and hydrolyzing α-amylase and α-glucosidase, as well as maintaining lower cellular glucose levels [20], [21]. Several bioactive compounds, such as phenolics, polysaccharides, and vitamin C, have been shown to lower blood glucose levels and act as antioxidants that support the prevention of diabetes mellitus [22]-[24]. A promising new source for development as an antidiabetic and antioxidant therapy is the non-edible parts (huks) of wild durian from Sabah, namely Durian Sukang *(Durio oxleyanus)*.

Various studies on the use of durian husk and seeds from a number of regions have been conducted. For example, [25] used ethanol extract of durian husk obtained from Surakarta, Central Java, and found that the extract had antidiabetic and antioxidant activities. Another study by Charoenphun and Klangbud [26], showed that ethanol extracts from Monthong and Chanee durian varieties from Thailand have antioxidant and anti-inflammatory effects. Furthermore, a recent study Muhtadi et al. [27], revealed that ethanol extracts from durian husk not only act as antioxidants and antidiabetics, but also have anticholesterol and antihyperuricemic activities. Durian husk is known to contain various secondary metabolites, including flavonoids such as catechin and quercetin [28] polyphenols [26] and tannins [29]. Although a number of studies have explored the potential of durian peel and seeds from various varieties and regions, most studies are still limited to ethanol extracts and conventional biological activity assays. Research that integrates LC-MS metabolite analysis with computational approaches such as molecular docking remains rare, particularly for endemic species such as *Durio oxleyanus* (Sukang durian) from Sabah.

The novelty of this study lies in the utilization of the inedible parts of *Durio oxleyanus* as a source of potential antidiabetic drugs through the integration of LC-MS analysis and molecular docking simulations. This approach not only confirms the role of flavonoids as inhibitors of starch hydrolysis but also introduces a new paradigm in drug discovery based on local biomass that was previously considered waste. By combining the exploration of endemic biodiversity with multi-target computational validation of key diabetes enzymes, this study presents an innovative and sustainable model for the development of natural medicines while supporting the concept of sustainable bioprospecting.

This study was motivated by the need for diabetes therapies that are safer, more affordable, and more environmentally friendly than synthetic drugs. The primary objective of the study is to explore the bioactive potential of hydroalcoholic extracts of *Durio oxleyanus* as inhibitors of α-glucosidase and α-amylase using a computational approach. The results of this study are expected to contribute to the discovery of new sources for the development of innovative and sustainable antidiabetic drugs.

2. RESEARCH METHOD

2.1. Material and Method

Sample Preparation and Extraction

Sukang durian husk (*Durio oxleyanus*) was collected from the tropical forests of Sabah, Malaysia. It was cleaned with running water and dried at room temperature (~25–30°C) for 5–7 days. Once dry, the samples were ground using a stainless steel blender (Japan) to produce a powder. The extraction process of *Durio oxleyanus* used a mixture of methanol and water in a ratio of 7:3 (v/v). The *Durio oxleyanus* huks samples were extracted in a shaker at a speed of 100 rpm and a temperature of 50 °C for 24 hours. The extract was filtered using filter paper (Whatman No. 5). The extract was concentrated employing a rotary evaporator under reduced pressure. This process aims to more optimally dissolve polar and semi-polar bioactive compounds that have potential biological activity, including phenolic and flavonoid compounds[17].

2.2. LC-MS analysis

Liquid Chromatography Conditions

The spectrometric analysis of DHHAE was carried out using an Agilent LCMS-IT-TOF model at the Centre for Instrumentation and Science Services, UMS. The proposed analytical conditions (with potential modifications and adaptations) for the liquid chromatography were as follows: LC column: Shimadzu SB-C18 (1.8 µm, 2.1 mm × 100 mm); the mobile phase consisted of pure water with 0.1% formic acid and acetonitrile with 0.1% formic acid. Sample measurements were performed using a gradient program, with parameters such as flow rate and temperature appropriately controlled.

IT-TOF MS

Fragmentation was carried out using an IT-TOF-MS mass spectrometer equipped with an ESI source in negative ionization mode. The analytical MS parameters were optimized as follows: interface voltage −3.5 kV; nebulizing gas (N_2) flow, 1.5 L/min; drying gas pressure, 50 kPa; ion trap pressure, 1.7×10^{-2} Pa; ion accumulation time, 30 ms; and the isolation width of precursor ions, 3.0 amu. Accurate mass determination was corrected by calibration using sodium trifluoroacetate as a reference. Ultra-high purity argon was used as both the cooling and collision gas for collision-induced dissociation (CID), and the collision energy was set between 50%–100%. The raw data files obtained from the IT-TOF-MS runs were converted to vendor-independent NetCDF (Network Common Data Format) files. MZmine software version 2.23 (http://mzmine.github.io) was applied for data processing. MZmine processing consisted of several stages, including input file manipulation, spectral filtering, peak detection, chromatographic alignment, normalization, visualization, and data export, each controlled by specific parameters. These processes ensured that only mass fragments produced due to the presence of metabolites were utilized for mass identification, excluding background noise. The Find Molecular Formula Algorithm (MFG) software was used for molecular formula prediction based on mass fragmentation. For compound identification, the NIST MS Search v.2.3 (2017) software with the NIST 17 EI Library Version was utilized.

2.3. Molecular Docking Analysis

Laptop specification : Intel(R) Core(TM) Ultra 5 225H (1.70 GHz) and 16,0 GB (15,4 GB usable) of Random-Access Memory (RAM), along with several software, namely AutoDocktools-1.5.7, pyRx 0.8. The ligand structures were constructed using ChemDraw Professional 15.0 software, Chem3D 15.0, PyMol 3.0 and BIOVIA Discovery Studio Visualizer. All software was run on the Windows 11 operating system.

Protein Selection: 3D crystal structures protein downloaded from the Protein Data Bank (PDB) (www.rcsb.org) Ligand Selection: The materials used were 3D structures of LC-MS result from Husk Hydro-Alcoholic extract (DHHAE) downloaded from the PubChem database (https://pubchem.ncbi.nlm.nih.gov/)

Ligand Preparation

The 3D structures of ligands identified by LC-MS from the hydro-alcoholic extract of *Durio oxleyanus* (DHHAE) were downloaded from the PubChem database (https://pubchem.ncbi.nlm.nih.gov/ in .sdf format. These structures were created using ChemDraw Professional 15.0 and then optimized with Chem3D 15.0 using the MMFF94 (Merck Molecular Force Field) method to minimize energy and improve geometry. The optimized file was saved again in .sdf format for use in the docking process.

Protein Preparation

The 3D crystal structures of the target proteins, namely α-glucosidase (PDB ID: 2QMJ) and α-amylase (PDB ID: 1B2Y), were obtained from the Protein Data Bank (www.rcsb.org) in .pdb format. Protein preparation was performed by:

1. Removing water molecules and native ligands using BIOVIA Discovery Studio Visualizer.
2. Adding polar hydrogen atoms and Gasteiger charges using AutoDockTools 1.5.7.
3. The prepared protein files were saved in .pdbqt format for the docking process.

Docking Procedure

The docking process is performed using PyRx 0.8 software that integrates AutoDock Vina as a bond affinity calculation engine [18]. The prepared target protein molecules are entered into PyRx, where the ligands undergo energy minimization using open babel menu. Docking begins by

1. opening the vina wizard menu
2. Select the protein and ligand by pressing Ctrl + click.
3. Click Forward → set the grid box (based on the native ligand position; the smaller the grid box, the more accurate the docking will be).
   2QMJ grid box : center_x = -21.747, center_y = -6.245, center_z = -5.397, size_x = 9.696, size_y = 7.335 size_z = 17.155
   1B2Y grid box = center_x = -4.386, center_y = 15.891, center_z = 32.720, size_x = 85.038, size_y = 63.733, size_z = 83.444
4. Set the exhaustiveness parameter = 8 (Vina default can be increased for higher accuracy).
5. Perform the docking process 3 times to ensure consistency of results.
6. Click Forward to start the docking process and save the results in .pdb format.

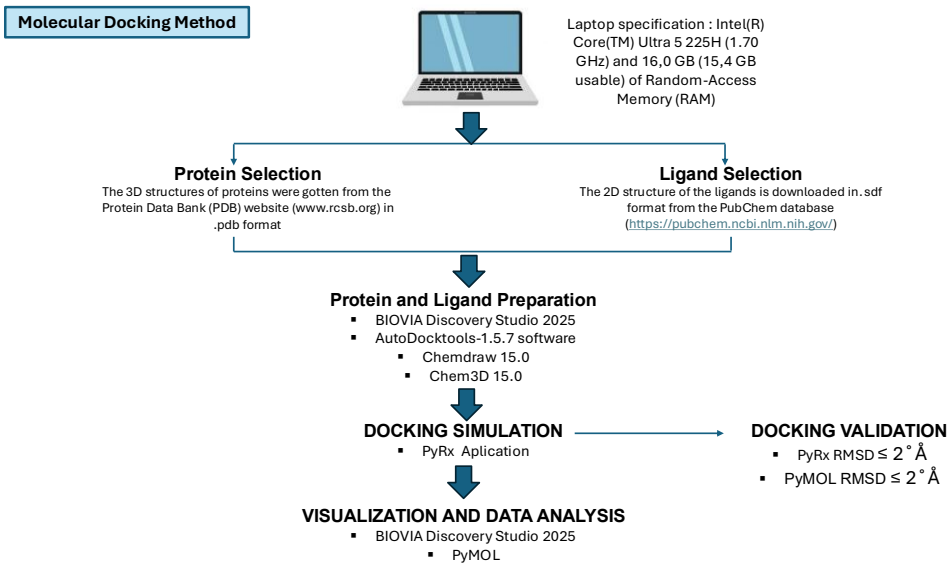

Figure 1 : Molecular docking process

Docking Validation

Validation was performed by redocking the previously separated native ligand. The goal was to ensure that the docking protocol was valid with an RMSD ≤ 2 Å.

1. The best docking result was selected based on an RMSD lower bound and an RMSD upper bound of ≤ 2 Å.
2. The file containing the best docking result was visualized alongside the native ligand using PyMOL 3.0.
3. The RMSD was calculated using the command:
   "align (obj1), (obj2), cycles=0, transform=0"
4. The method is considered valid if the RMSD value is less than ≤ 2˚Å and Match: assigning 1 x 1 pairwise scores.

Visualization

Visualization of ligand-protein interactions was performed using PyMOL 3.0 and BIOVIA Discovery Studio Visualizer to display:

1. The ligand's position within the protein's active site.
2. The types of bonds (hydrogen, hydrophobic, electrostatic).
3. Key residues that interact with the ligand.

3. RESULTS AND DISCUSSION

3.1. Extraction Sample

The hydroalcoholic extraction process was performed exclusively on *Durio oxleyanus* husk using a methanol-water mixture at a ratio of 7:3 (v/v). This solvent system was deliberately selected for its well-established efficacy in dissolving both polar and semi-polar bioactive compounds, particularly phenolic acids, flavonoids, glycosides, and condensed tannins, which collectively exhibit higher biological activity potential [30]–[32]. The methanol-water combination offers broader solvation capacity compared to single-solvent systems, enabling more comprehensive recovery of structurally diverse secondary metabolites, as subsequently confirmed by LCMS metabolite profiling in the present study.

The hydroalcoholic extraction yielded approximately 8.3% (w/w) of dry extract, a value consistent with the high-polarity solvent system employed, which favors co-extraction of both hydrophilic and moderately lipophilic phytochemicals. The resulting extract presented as a dark brown, hygroscopic powder with a characteristic aromatic odor and a slightly bitter taste. The dark coloration is attributable to the abundant polyphenolic and flavonoid constituents identified in this study, including catechins, procyanidins, and quercetin derivatives, while the hygroscopicity and moderate aqueous solubility are reflective of the co-presence of polar glycosidic conjugates and organic acids, namely gluconic acid and citric acid, within the extract matrix.

The use of hydroalcoholic solvents has been demonstrated to produce a more diverse phytochemical spectrum compared to aqueous extraction alone [33], with solvent composition shown to exert a significant influence on both the yield and qualitative profile of extracted compounds [34]. Methanol-water was specifically selected over ethanol-water in the present study to achieve higher extraction efficiency, improved reproducibility, and enhanced recovery of flavonoids and phenolic acids. Protic polar media such as hydroalcoholic solutions are particularly effective for extracting phenolic compounds with high antioxidant activity, as highlighted by Rodrigues et al. [34, [35]. Furthermore, precise adjustment of extraction parameters, including temperature, solvent concentration, extraction duration, and the material-to-solvent ratio, has been confirmed to improve bioactive component isolation efficiency and optimize therapeutic outcomes in biological models [36].

3.2. LC-MS Analysis

To further characterize the phytochemical composition of DHHAE, Liquid Chromatography–Mass Spectrometry (LC-MS) analysis was performed. This technique enables the separation, detection, and identification of bioactive compounds based on their retention time, mass-to-charge ratio, and spectral characteristics. LC-MS is widely used in natural product research to profile secondary metabolites, particularly phenolic compounds and flavonoids, which are known to contribute significantly to the biological activities of plant extracts. The chromatographic profile obtained provides valuable information regarding the diversity and relative abundance of phytochemical constituents present in DHHAE. The LC-MS chromatogram is presented in Figure 2.

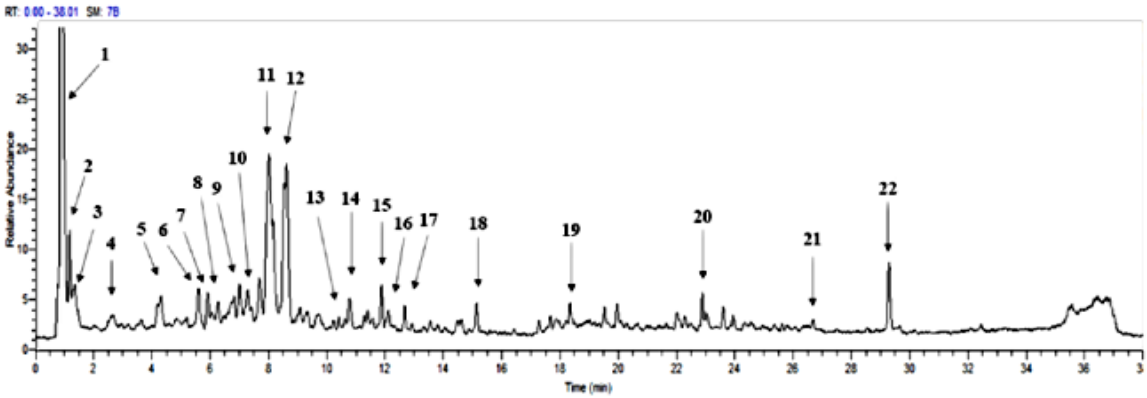

Figure 2. LC-MS result

LCMS analysis (Figure 1) revealed the presence of various important phenolic compounds and flavonoids in DHHAE. Compound identification is based on a combination of RT, maximum wavelength (Max Wave), and molecular formula. Compounds with RT values consistent with their polarity, characteristic UV spectra (e.g., flavonoids with strong absorption at 280–320 nm), and molecular formulas that match literature data can be identified with a high degree of confidence. The main compounds identified include caffeic acid, gluconic acid, citric acid, protocatechuic acid, quercitrin, sinapic hexoside, malvidin-3-O-glucoside, catechin, type B procyanidin, rutin, quercetin-3-O-glucoside, and kaempferol-rhamnoside. These compounds are known to have

antioxidant, antidiabetic, and various other bioactive effects. Peak intensity reflects the relative concentration of a compound. Compounds with sharp, high peaks, such as catechin and rutin, can be considered the major components of the extract. Compounds with lower intensity, such as vanillic acid-O-hexoside or protocatechuic acid-O-hexoside, are likely minor metabolites, but remain relevant because they may contribute to synergistic effects.

Retention time (RT) indicates how long it takes for a compound to elute from the chromatographic column. Polar compounds such as caffeic acid, gluconic acid, and citric acid elute earlier (RT < 1 minute), indicating high mobility. Conversely, complex compounds such as kaempferol-rhamnoside (RT 26.63 minutes) and lucidenic acid D1 (RT 15.14 minutes) have longer retention times, indicating stronger interactions with the stationary phase due to hydrophobic properties or larger molecular size. Peaks with longer retention times (e.g., rutin at 10.36 minutes and procyanidin B at 7.19 minutes) typically indicate compounds with high relative abundance, due to their greater peak intensity. Flavonoid compounds such as rutin, quercetin, catechin, and procyanidin B appear to be dominant, confirming that the peel of *Durio oxleyanus* is rich in secondary metabolites with bioactive properties.

Table 1. Spectrum of DHHAE LC-MS Result

Peak No	Identification	RT (min)	Max Wave	Mol.Formula
1	Caffeic acid	0.8	280	$C_9H_8O_4$
2	Gluconic acid	0.9	280.32	$C_6H_{12}O_7$
3	Citric acid	0.89	280	$C_6H_8O_7$
4	protocatechuic acid-O-hexoside	2.64	320	$C_{13}H_{16}O_9$
5	Quercetin	4.3	280.32	$C_{21}H_{20}O_{11}$
6	sinapic acid hexoside	5.61	280	$C_{17}H_{22}O_{10}$
7	Malvidin-3-o-glucoside	5.95	280.32	$C_{23}H_{25}O_{12}$
8	Cathecin	6.21	280.32	$C_{15}H_{14}O_6$
9	ProcyanidinB	7.19	280.32	$C_{30}H_{26}O_{12}$
10	Quercetin-3-O-rhamnoside	7.69	320	$C_{21}H_{20}O_{11}$
11	Rutin	10.36	280.32	$C_{27}H_{30}O_{16}$
12	Quercetin-3-o-glucosidase	10.75	280.32	$C_{21}H_{20}O_{10}$
13	Quercetin-3-O-glucuronide	12.05	280.32	$C_{21}H_{20}O_{11}$
14	Lucidenic acid D1	15.14	320	$C_{27}H_{34}O_7$
15	Vanillic acid-O-hexoside	18.71	280.32	$C_{14}H_{18}O_9$
16	kaempferol-rhamnoside	26.63	320	$C_{21}H_{35}O_9$

The MS/MS fragmentation spectrum (Table 1) provides confirmatory evidence for the structure of a number of important compounds. In procyanidin B, characteristic fragment ions were detected at m/z 425.1506, 287.0889, and 533.2301, indicating the loss of the $C_7H_4O_4$ and $C_{13}H_{10}O_6$ groups. The catechin spectrum shows a main fragment at m/z 245.0854 due to the release of the CO_2 group. Meanwhile, quercitrin produced a dominant ion at m/z 301.0461 originating from the breakdown of the rhamnoside group, while quercetin-3-O-glucoside displayed a fragment at m/z 300.0973 through the release of the glycoside group. Research by Tran et al. [5], also reported that HPLC results of durian husk extract *(Durio zibethinus Murr)* from Vietnam showed the highest quercetin content. Additionally, a study by Khaksar et al. [31], identified that durian husk generally contains various bioactive compounds, including phenolic acids and phenolic glycosides, coumarins, triterpenoids, simple glycosides, pectins, and flavonoids [32]-[36]. Overall, these results prove that DHHAE is rich in polyphenolic compounds, flavonoids, and organic acids that play an important role in antidiabetic and antioxidant activities.

3.3. Molecular Docking Analysis

To investigate the molecular interactions between the identified phytochemical compounds and key antidiabetic targets, molecular docking analysis was performed using α-glucosidase and α-amylase enzymes. These enzymes were selected because they are directly involved in carbohydrate digestion and glucose release in the human body. The three-dimensional (3D) structures of both target proteins were retrieved from the Protein Data Bank (PDB) and prepared for docking studies. Visualization of the protein structures is presented in Figure 3

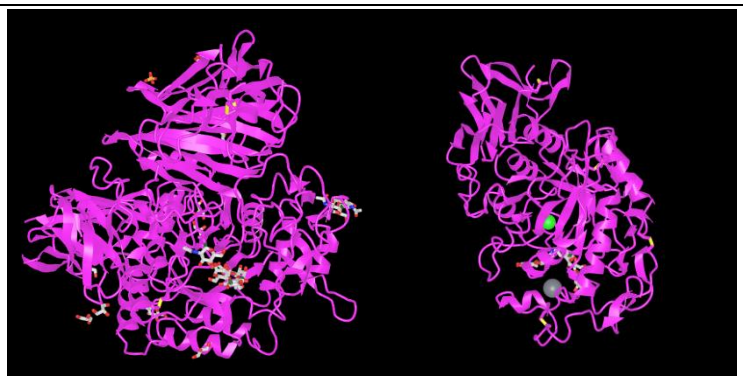

A B

Figure 3. 3D of alpha-glucosidase protein (PDB:2QMJ) and alpha-amylase (PDB:1B2Y)

The enzymes α-glucosidase (PDB: 2QMJ) and α-amylase (PDB: 1B2Y) were chosen because they play central roles in carbohydrate digestion. α-Glucosidase hydrolyzes terminal α-(1→4) glycosidic bonds in disaccharides and oligosaccharides, producing glucose for absorption, while α-amylase catalyzes the breakdown of starch into maltose and glucose. Inhibiting these enzymes is a well-established therapeutic strategy for controlling postprandial hyperglycemia in type 2 diabetes, making them highly relevant pharmacological targets.

Active Site of Protein Target

The active site of the α-glucosidase protein (PDB: 2QMJ) is a binding pocket where carbohydrate substrates interact before being cleaved. The mechanism of action of this active site is determined by the key catalytic residues, namely aspartate (Asp203 and Asp542) and arginine (Arg526), which play a direct role in the cleavage of glycosidic bonds through hydrogen bonding and hydrophobic interactions. In addition, the active site of NtMGAM has two binding subsites: the first subsite serves as the binding site for the glycon, while the second subsite serves as the binding site for the aglycone. In the 2QMJ crystal structure, acarbose, as a natural ligand, occupies the active site pocket by mimicking the structure of a sugar, thereby blocking the entry of natural substrates and preventing the hydrolysis process. This mechanism explains how acarbose acts as an α-glucosidase inhibitor and forms the basis for enzyme-inhibition strategies aimed at lowering blood glucose levels in people with diabetes.

The active site of the α-amylase enzyme (PDB: 1B2Y) is located within a deep cleft in Domain A, with a folded structure consisting of an α/β barrel containing eight strands. In this structure, acarbose, a natural inhibitor, binds directly to the active site, thereby inhibiting the breakdown of complex carbohydrates into glucose. The active site is an elongated pocket with at least five binding subsites (from -3 to +2) that serve to accommodate the sugar chains of the starch being processed. Within this pocket are three highly conserved key catalytic residues: Asp197, which acts as a nucleophile attacking the α-1,4 glycosidic bond; Glu233, which serves as a proton donor to cleave the sugar bond; and Asp300, which stabilizes the charge and aids in substrate orientation during the hydrolysis reaction. This active-site activity is also influenced by the stabilizing cofactor environment: calcium ions (Ca^{2+}), which maintain the structural integrity of Domains A and B, and chloride ions (Cl^{-}), which bind to residues Arg195, Asn298, and Arg337 around the catalytic pocket to modulate charge, thereby enhancing substrate processing efficiency. This structure explains how α-amylase functions optimally in breaking down starch, as well as how acarbose is able to inhibit its activity as a therapeutic strategy for diabetes.

Native Ligand Comparison

In both target proteins (2QMJ and 1B2Y), the docking protocol was benchmarked against their native ligands to ensure accuracy. For α-glucosidase (2QMJ), acarbose occupies the active site and mimics carbohydrate substrates, providing a reference for evaluating the binding orientation of test ligands. For α-amylase (1B2Y), acarbose also serves as the native inhibitor, allowing direct comparison of docking scores and interaction profiles. The ability of the docking program to reproduce the native ligand's binding pose and interactions validates the reliability of the docking setup.

Docking Reliability Discussion

Docking reliability was supported by consistent RMSD values below 2 Å, confirming that the redocking process successfully reproduced native ligand orientations. The alignment scores and atom overlaps further strengthen confidence in the docking protocol. By validating against native ligands, the docking workflow demonstrates reproducibility and accuracy in predicting binding modes. Nevertheless, docking remains a computational prediction; therefore, complementary molecular dynamics simulations and experimental enzyme assays are required to confirm the stability and biological relevance of the predicted interactions.

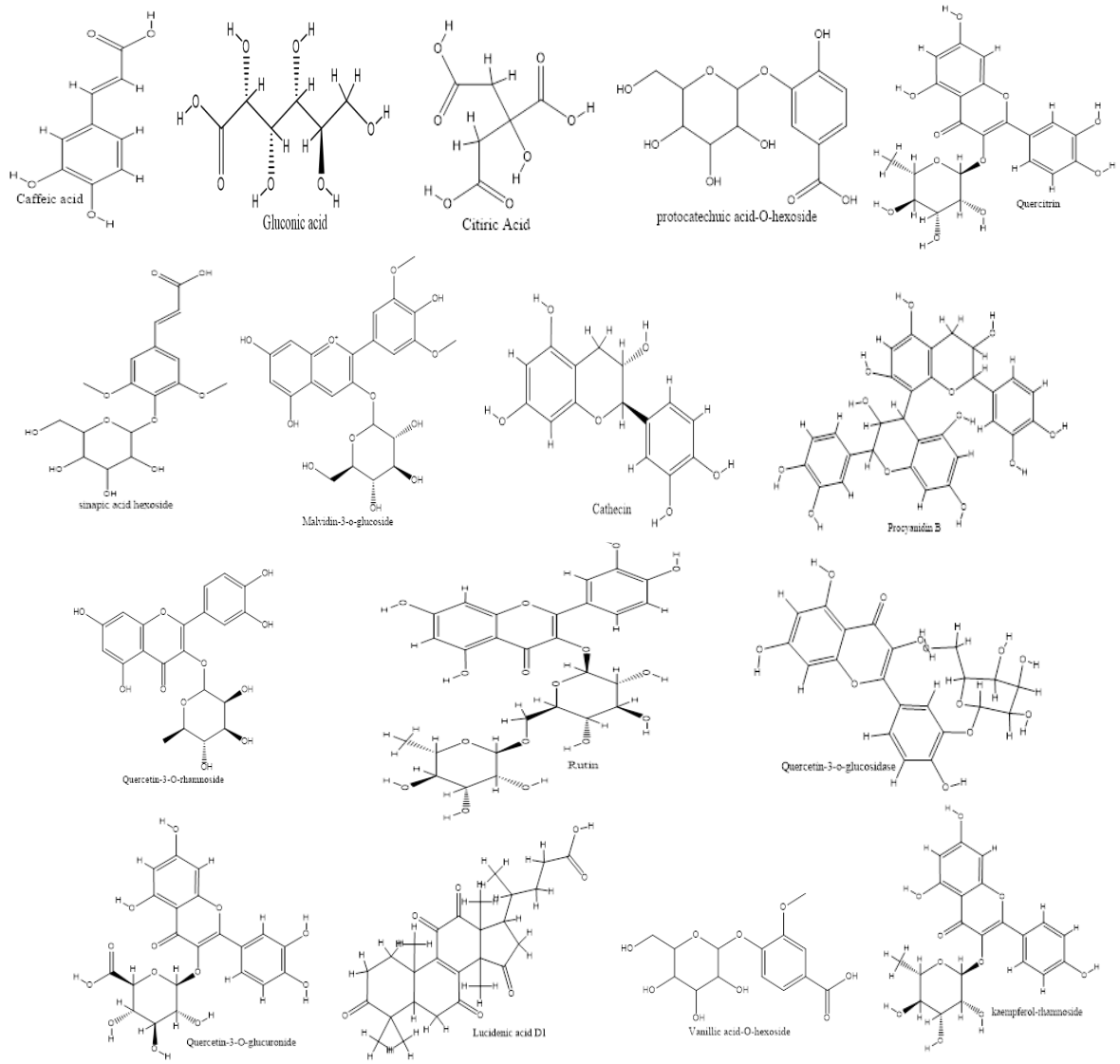

Figure 4. 2D of the Ligand from *Durio oxleyanus* Hydro-Alcoholic extract (DHHAE)

Redocking Result Native Ligand

The parameters analyzed were the lower and upper RMSD values obtained after redocking the original ligand with the protein using the PyRX application. The best results were achieved when both RMSD values were below 2 Å. RMSD itself is used to assess the degree of difference in ligand position before and after redocking [25] Further validation on protein 2QMJ using the PyMOL application showed the successful alignment of 58 atoms from two structures, resulting in an alignment score of 5,000 with an RMSD of 1.624 Å. Meanwhile, protein 1B2Y gave an alignment score of 5,000 with an RMSD of 0.967 Å. RMSD describes the similarity of atom positions between two structures after the alignment process; the smaller the value, the higher the level of similarity. A value of 1.624 Å indicates fairly good conformity, as an RMSD < 2 Å is generally considered valid (Zhang et al., 2016). Thus, the same grid box dimensions and coordinates can be used for docking the test ligand. Figure 3 shows a comparison of the original 2QMJ and 1B2Y ligands before and after redocking.

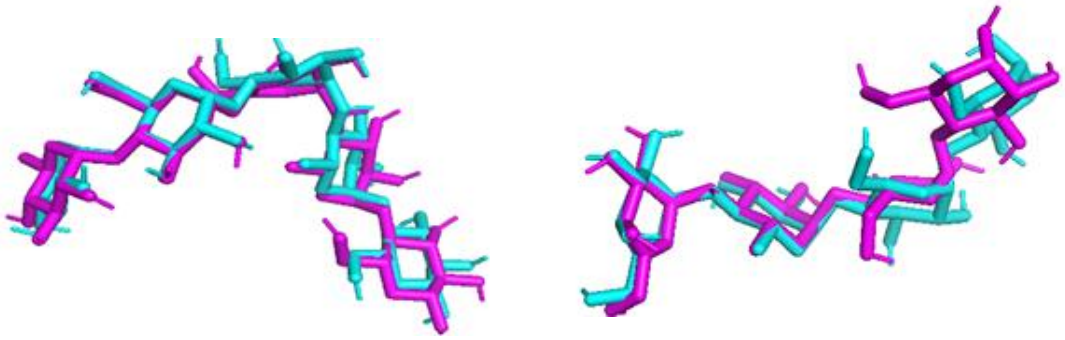

(a) 2QMJ **(b) 1B2Y**

Figure 5. Overlay of native ligand before (blue) and after (purple) redocking

3.4. Interactions of the Ligands with α-glucosidase Amino Acid Residues

In the docking simulation process, each ligand tested will produce a Gibbs free energy value (ΔG). This value reflects the amount of energy involved when the ligand interacts with the receptor [39]. The lower the ΔG value, the stronger the bond formed and the greater the likelihood of the reaction occurring spontaneously [40]. This condition occurs because energy is released during complex formation, so that the free energy of the system after the ligand and receptor bind is lower than before the interaction occurred.

In this study, molecular interactions between the target protein 2QMJ and a number of potential ligands were analyzed based on binding affinity values (ΔG), interacting amino acid residues (hydrogen bond, hydrophobic bond and electrostatic), and interatomic distances in angstroms (Å). Hydrogen bonds play a fundamental role in ligand-receptor binding because they direct the ligand to the correct position within the active site and help maintain the molecule's orientation. The relatively short bond length (approximately 2–3 Å) allows for strong interactions with polar or charged residues, thereby increasing the binding energy and stabilizing the complex. On the other hand, hydrophobic interactions make a significant contribution to overall stability by displacing water molecules from the binding pocket and facilitating aromatic stacking effects, particularly in residues such as PHE575 or TRP406. These interactions not only enhance binding affinity but also improve the conformational fit between the ligand and the receptor. Electrostatic interactions also play a crucial role in the interactions between charged groups on the ligand and charged residues on the protein, such as ASP or GLU (negative) with ARG or LYS (positive). These interactions enhance binding affinity, help direct the ligand's orientation to the correct position within the binding pocket, and increase the specificity of the complex. Ultimately, electrostatic interactions serve as a key factor that complements the roles of hydrogen and hydrophobic bonds in forming stable and selective ligand-receptor complexes.

The docking results (Table 2 and Figure 5) show that catechin has the strongest binding affinity with ΔG -7.1 kcal/mol, interacting hydrogen bond closely with the ASP203 residues at a distance of <3 Å, thus having high potential as an inhibitor. Rutin also exhibits high affinity (ΔG = -6.9 kcal/mol) through multipoint hydrogen bond interactions with THR205, ARG526, ASP203 and ASP327, indicating complex and stable binding ability. Quercetin-3-O-glucosidase exhibits lower affinity (-6.4 kcal/mol), although it still interacts with key residues such as THR205, ARG526, and ASP443. Hydrophobic interactions with TYR299, TRP406, and PHE575 also stabilize the bond, but the overall strength remains lower than that of Catechin and Rutin.Meanwhile, Lucidenic acid D1 and Vanillic acid-O-hexoside exhibit moderate affinity (-6.7 kcal/mol), with distinct interaction patterns. Lucidenic acid D1 forms only simple hydrogen bonds with THR205 and ARG526, whereas Vanillic acid-O-hexoside exhibits more hydrogen bonds, involving ASP307, ASP203, and ASP542, as well as hydrophobic interactions with TRP406.

Overall, this analysis confirms that residues THR205, ARG526, ASP203, ASP542, TRP406, and PHE575 are key hotspots for ligand binding at the 2QMJ receptor. Cathechin stands out as the leading candidate with the strongest affinity, while Rutin offers advantages in the number and variety of interactions that can enhance complex stability. These findings are in line with the research by Elhady et al.[41], who used compounds from *Aspergillus terreus* as α-glucosidase inhibitors in silico with autodockvina on the 2QMJ protein, where the ASP, ARG, and HIS residues were also involved. Similar results were obtained in a study by Januarto [42] on stevioside compounds from *Stevia rebaudiana*, which showed interactions with the same residues in the 2QMJ protein.

Table 2. Interactions of the best ligands with α-glucosidase Amino Acid Residues

Receptor	Binding affinity (ΔG)	Ligand	Interacting amino acid			
			Hydrogen Bond	Hydrogen Bond Distance (Å)	Hydrophobic Interaction	Electrostatic
2QMJ	-7,1	Cathecin	ASP203	2,31 Å	PHE575	ASP443
	-6,9	Rutin	THR205, ARG526, MET444, ASP327, ASP203	2,85 Å, 2,35 Å, 2,54 Å, 3,04 Å, 2,10 Å, 3,45 Å	TYR299, TRP406, PHE575	ASP9542
	-6,4	Quercetin-3-o-glucoside	THR205, ARG526, ASP443,	3,11 Å, 2,91 Å, 2,79 Å, 2,60 Å, 2,47 Å	TYR299, TRP406, PHE575	ASP542
	-6,7	Lucidenic acid D1	THR205, ARG526	2,71 Å, 3,03 Å		
	-6,7	Vanillic acid-O-hexoside	THR205 ASP307, ASP203, ASP542	2,82 Å, 2,77 Å, 2,27 Å, 1,94 Å, 3,45 Å, 2,88 Å	TRP406	ASP542

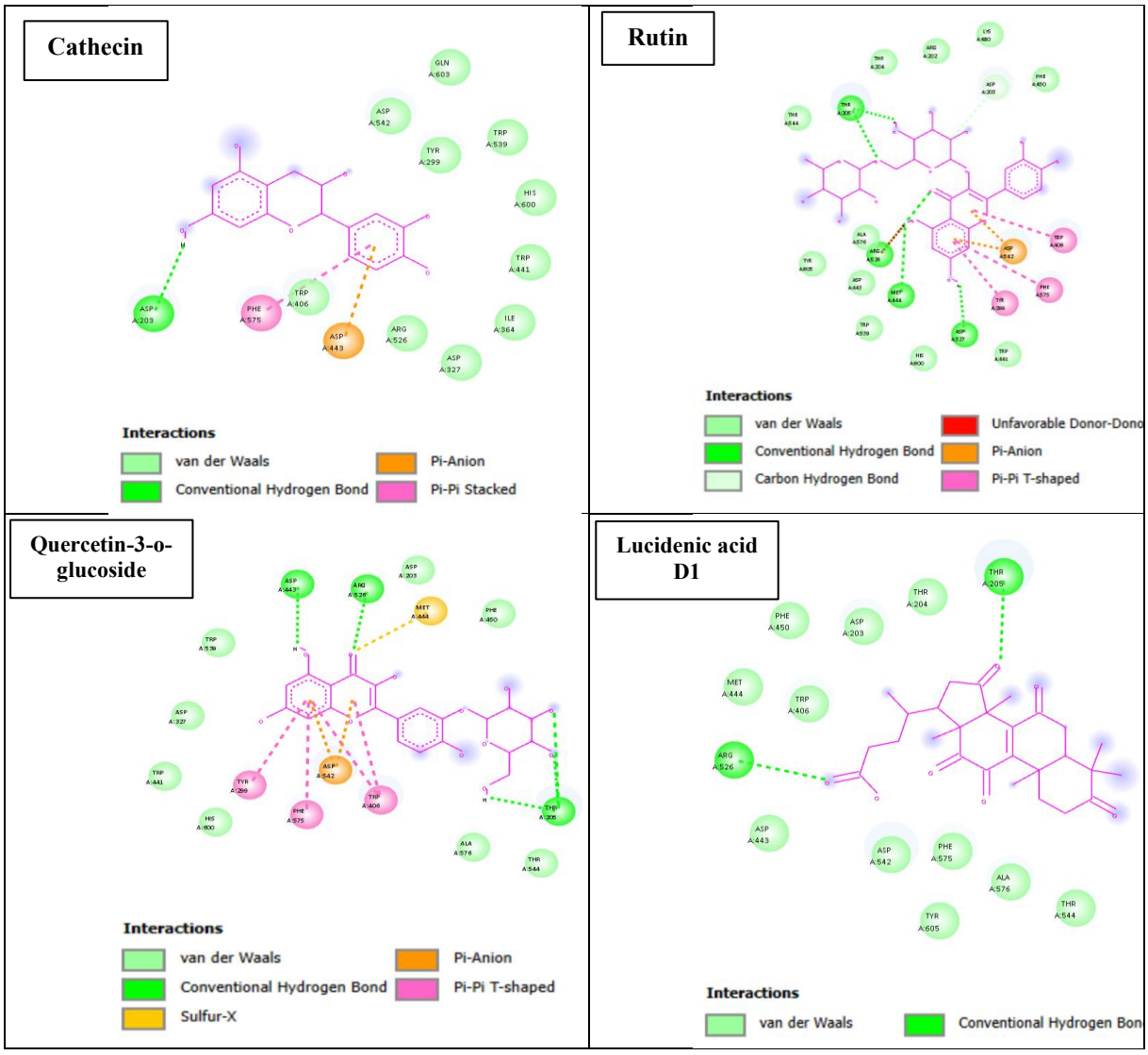

Figure 6. Interactions visualization of 2QMJ receptor with the best Ligands

Docking Simulation Visualization 2QMJ

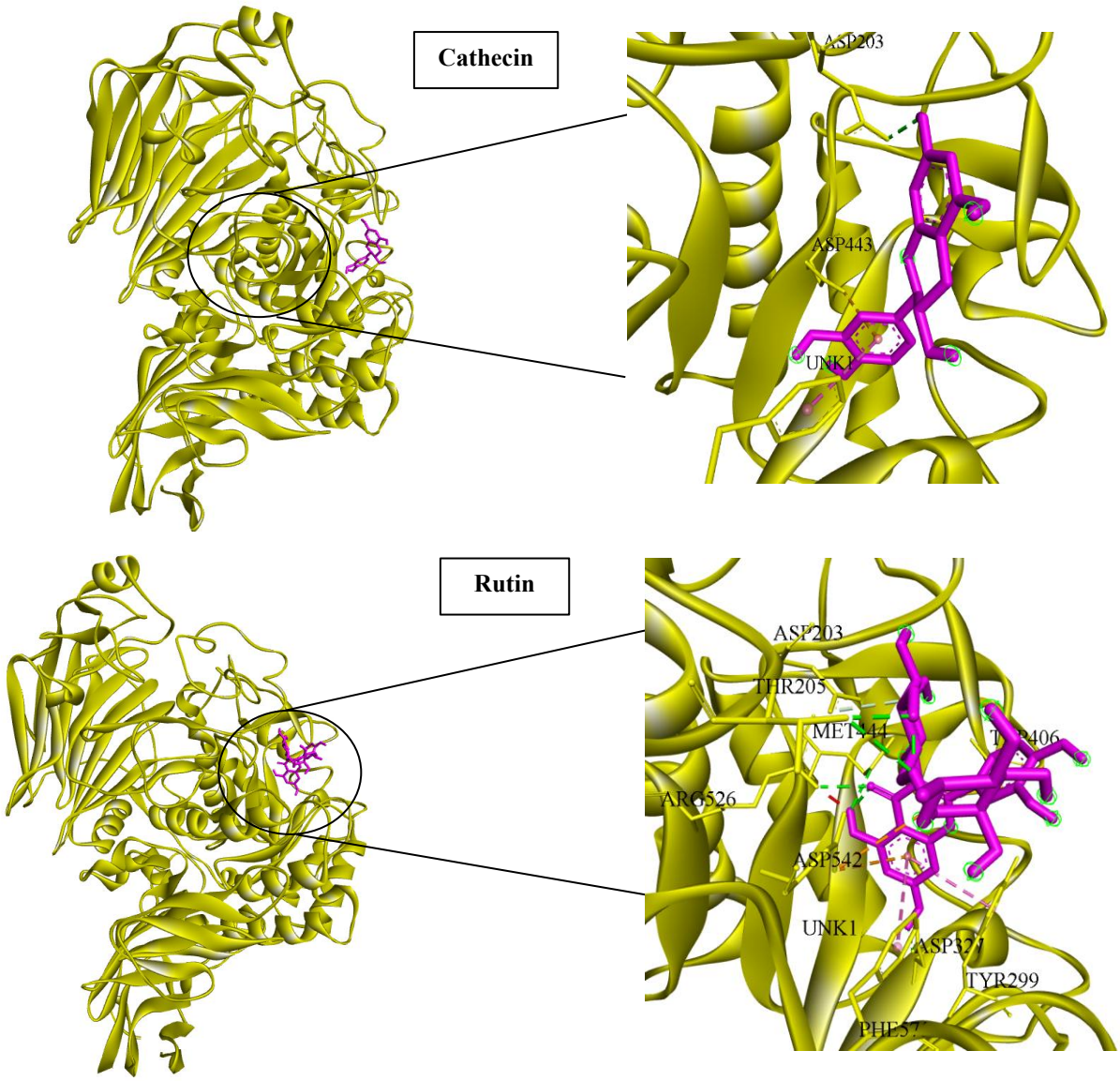

Figure 7. Docking visualization of 2QMJ receptor with Cathecin and Rutin Ligands

The results of the docking simulation provide important insights into the potential mechanism of enzyme inhibition by the tested ligands against the 2QMJ target protein. Strong hydrogen bonds, such as those formed by catechin with residue ASP203 and by rutin with THR205, ARG526, and ASP327, indicate the ligands' ability to compete with the natural substrate at the catalytic site. By occupying and stabilizing key residues in the active site, ligands can disrupt substrate orientation and reduce the enzyme's catalytic activity, thereby producing an inhibitory effect.

Hydrophobic interactions with residues such as TRP406 and PHE575 further enhance ligand stability within the binding pocket. These interactions displace water molecules and facilitate aromatic stacking effects, ensuring that the ligand remains firmly bound and is difficult for the substrate to displace. Meanwhile, electrostatic interactions with charged residues, such as ASP542 and ARG526, provide additional specificity by directing the ligand into the correct orientation and enhancing binding affinity. The combination of hydrogen bonding, hydrophobic, and electrostatic interactions underscores the potential of catechins and rutin as strong and selective inhibitor candidates. The identification of hotspot residues (THR205, ARG526, ASP203, ASP542, TRP406, and PHE575) strengthens the evidence that these ligands can modulate enzyme activity by blocking access to the catalytic site or altering protein conformational dynamics.

3.5. Interactions of the Ligands with α-amylase Amino Acid Residues

The results of molecular docking analysis on the 1B2Y protein show various interactions between ligands and active residues at the protein binding site (Table 3 and figure 7). The assessment was based on binding affinity values (ΔG), interacting amino acid residues (hydrogen bond, hydrophobic bond and electrostatic), and interatomic distances in angstroms (Å) which together describe the strength and stability of the complex formed. Lucidenic D1 is recorded as having the highest binding affinity with an energy ΔG of -9.8 kcal/mol. This ligand forms several hydrogen bonds with residues THR163, LYS200, HIS201, and GLU240, indicating stable and diverse interactions. This very low affinity suggests that Lucidenic acid D1 has the potential to be an effective inhibitor. Rutin also exhibits high affinity with a ΔG of −9.6 kcal/mol. This ligand interacts via multipoint hydrogen bonds with residues GLN63, LYS200, TRP59, and ASP197. This complex interaction pattern enhances the stability of the ligand–receptor complex, while the involvement of TRP59 and ILE235 residues adds a significant hydrophobic contribution. Thus, rutin can be considered a strong candidate due to its combination of low affinity and multipoint interactions that support bond stability.

Meanwhile, quercetin-3-O-glucosidase has a ΔG of -9.1 kcal/mol, which is slightly higher than that of rutin and lucidenic acid D1, but still exhibits extensive interactions. This ligand forms hydrogen bonds with residues GLN63, TYR62, TYR151, GLU233, and HIS305, as well as hydrophobic interactions with TRP59. In addition, the involvement of ASP300 in electrostatic interactions enhances the bond strength. This diverse pattern of interactions confirms that quercetin-3-O-glucosidase remains a relevant candidate as a potential inhibitor, even though its affinity is not as strong as that of rutin or Lucidenic acid D1. Catechin, with a ΔG of −8.9 kcal/mol, exhibits the lowest affinity among the ligands tested. However, this ligand still interacts with key residues such as GLU233 via hydrogen bonds, as well as TRP59 via hydrophobic interactions. The involvement of ASP197 and ASP300 in electrostatic interactions also contributes to the stability of the complex. Although the bond strength is weaker compared to other ligands, catechin still has potential as an inhibitor because it interacts with key catalytic residues.

Overall, the docking analysis results confirm that Lucidenic acid D1, Rutin, and Quercetin-3-o-glucosidase and cathecin are the main candidates with the potential to be further developed as bioactive agents against the 1B2Y protein. The interaction patterns involving polar residues (GLU, ASP, HIS), aromatic residues (TRP, TYR), and hydrophobic residues (LEU, ILE) are important indicators of the stability and specificity of the ligand bond with the target protein. Research by [31] on imidazo-isoxazole derivatives as alpha-amylase inhibitors also showed the involvement of polar residues ASP, HIS, and GLU in the 1B2Y protein. Meanwhile, a study by Fettach et al. [44], on thiazolidine-2,4-dione (TZD) compounds against the alpha-amylase enzyme (1B2Y) produced affinity energies ranging from -6.1 to -8.0 kcal/mol. Similar findings were observed in the compounds AN-153I105594 and AN-153I104845 from acarbose, which showed strong interactions with key alpha-amylase residues, such as TRP-59, GLN-63, GLU-233, and HIS-305 [45].

Table 3. Interactions of the best Ligands with α-amylase Amino Acid Residue

Receptor	Binding affinity (ΔG)	Ligand	Interacting amino acid			
			Hydrogen Bond	Hydrogen Bond Distance (Å)	Hydrophobic Interaction	Electrostatic
1B2Y	-8,9	Cathecin	GLU233	2,32 Å	TRP59	ASP197, ASP300
	-9,6	Rutin	GLN63, LYS200, TRP59, ASP197	2,89 Å, 3,14 Å, 2,17 Å, 2,47 Å	ILE235	
	-9,1	Quercetin-3-o-glucoside	GLN63, TYR62, TYR151 GLU233, HIS305	3,25 Å, 2,43 Å, 2,41 Å, 2,47 Å, 3,61 Å	TRP59	ASP300
	-9,8	Lucidenic acid D1	THR163, LYS200, HIS201, GLU240	3,06 Å, 2,69 Å, 3,10 Å, 2,40 Å	TYR62	

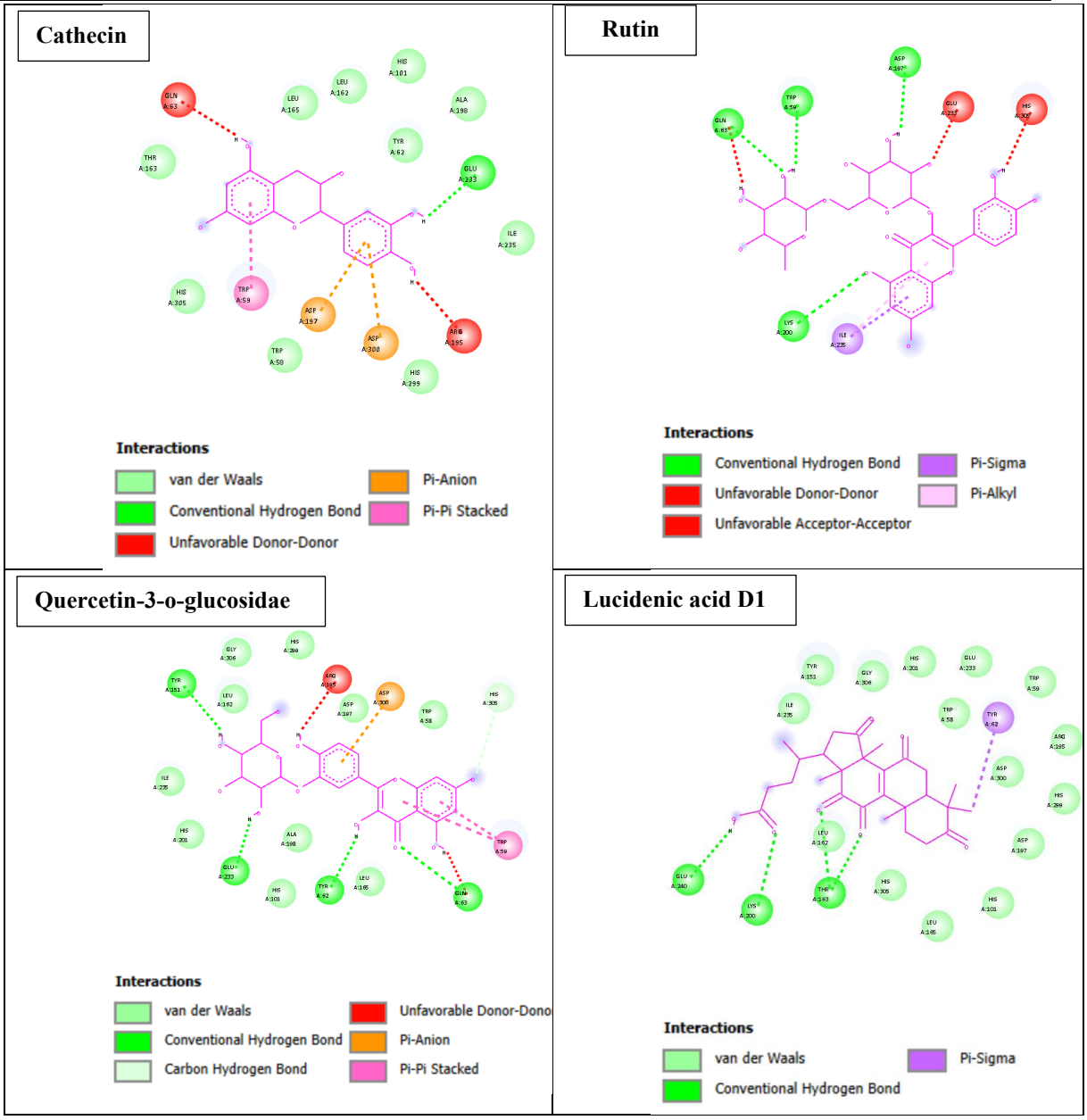

Figure 8. Interactions visualization of 1B2Y receptor with the best Ligands

Docking Simulation Visualization 1B2Y receptor

Docking analysis of the 1B2Y receptor indicates that ligands with low binding affinity (more negative ΔG) have great potential as enzyme inhibitors. Strong hydrogen bonds with catalytic residues such as GLU233, ASP197, and HIS305 can disrupt the orientation of the natural substrate, thereby inhibiting the enzyme's hydrolysis process. Hydrogen bonds act as anchors that position the ligand precisely within the active site, enabling the ligand to cover or block the substrate's access to the catalytic site. In addition, hydrophobic interactions with aromatic residues such as TRP59 and TYR62 play a key role in stabilizing the ligand within the binding pocket. This stability ensures that the ligand remains bound long enough to inhibit enzyme activity. Hydrophobic stacking also enhances the conformational fit of the ligand to the receptor, thereby increasing the effectiveness of inhibition.

Electrostatic interactions with negatively charged residues (ASP197, ASP300) or positively charged residues (LYS200) provide an additional contribution to affinity and specificity. These charges help direct the ligand into the correct orientation, making the bond more selective and stronger. Through a combination of hydrogen bonding, hydrophobic interactions, and electrostatic interactions, ligands such as Lucidenic acid D1 and Rutin have great potential to inhibit enzyme activity by blocking the active site or altering the protein's conformational dynamics. Biologically, this interaction means that the ligand can act as a competitive inhibitor, competing with the natural substrate for the binding site. When the ligand successfully forms a stable bond with a key residue, the enzyme loses its ability to bind and modify the substrate, resulting in a decrease in catalytic activity.

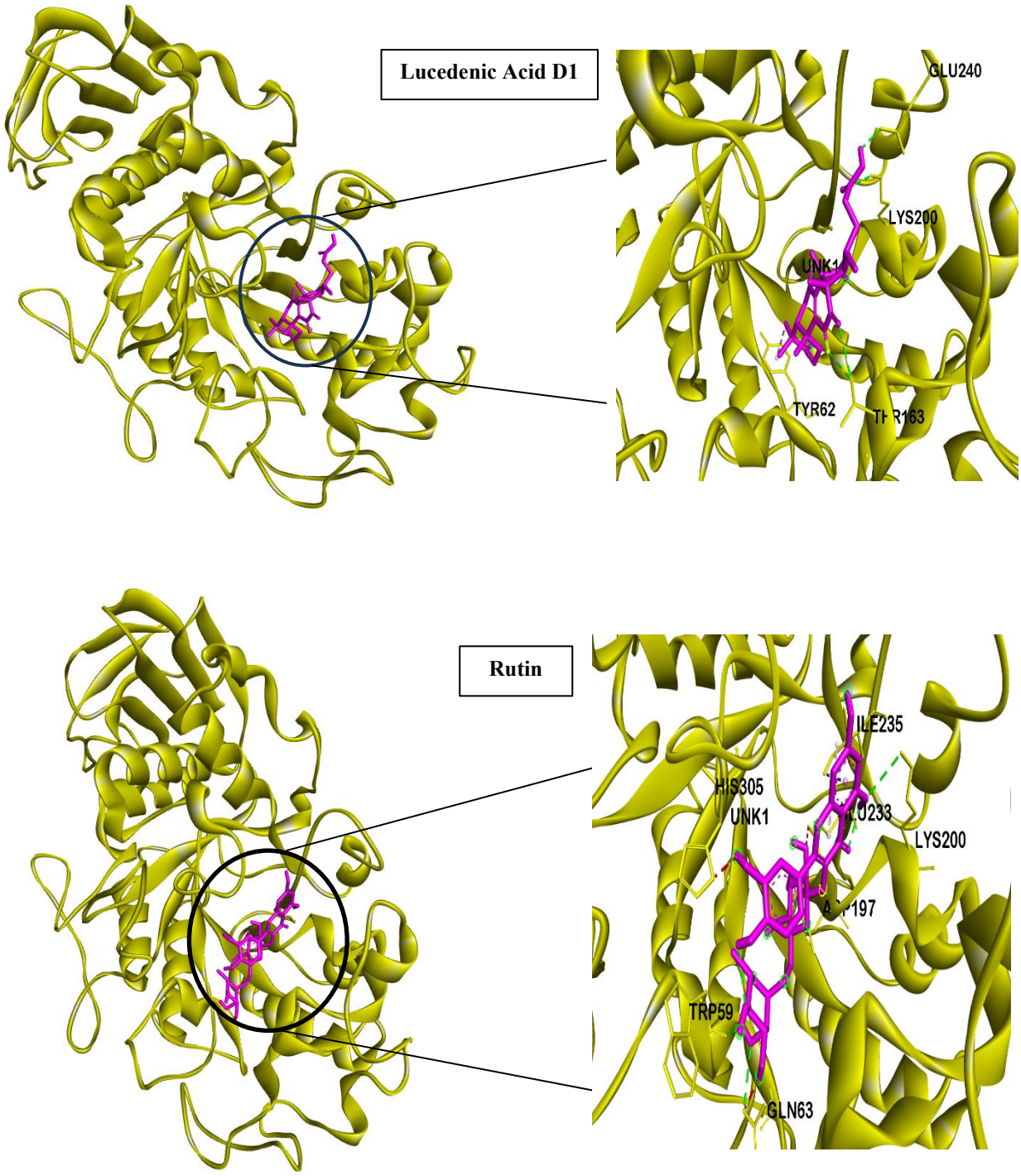

Figure 9. Docking visualization of 1B2Y receptor with Lucedenic acid D1 and Rutin Ligands

3.6. Analysis of Drug Properties and ADMET Prediction

The drug-likeness assessment based on Lipinski's Rule of Five was conducted to evaluate the oral bioavailability potential of the identified phytochemical compounds. Lipinski's criteria are widely used in early-stage drug discovery to predict the absorption and permeability characteristics of small-molecule drug candidates. The evaluated parameters included molecular weight (≤ 500 Da), lipophilicity (logP ≤ 5), hydrogen-bond acceptors (≤ 10), and hydrogen-bond donors (≤ 5). The results are presented in Table 4.

Table 4. Results of the analysis of drug-like properties based on Lipinski's rules

Ligand	Lipinski's rules			
	Molecular Weigh ≤ 500	MlogP ≤ 4,15 or logP ≤ 5	Hydrogen bond acceptor (nHA)≤ 10	Hydrogen-bond donor (nHD)≤ 5
Cathecin	290,271	1,173	6	5
Rutin	610,521	-1,137	16	10
Quercetin-3-o-glucoside	464,379	0,633	12	8
Lucidenic acid D1	470,562	3,287	6	1

The Lipinski Rule table above provides an overview of a compound's suitability as a candidate for an oral drug based on commonly used pharmacokinetic parameters. The catechin compound with a molecular weight of 290.271 Da, a logP value of 1.173, six hydrogen-bond acceptors, and five hydrogen-bond donors meets all Lipinski criteria, suggesting it has the potential for good bioavailability. However, another form of catechin with a higher molecular weight (610.521 Da) and a number of hydrogen-bond acceptors and donors that exceeds the limit exhibits limitations in permeability and absorption. Meanwhile, Quercetin-3-O-glucosidase exhibits two distinct profiles. In the first profile, the molecular mass of 464.379 Da, with 12 acceptors and 8 donors, exceeds Lipinski's rule, which may affect the compound's ability to penetrate cell membranes. Conversely, the second profile, with a molecular weight of 470.562 Da, a logP of 3.287, six acceptors, and one hydrogen bond donor, is more in line with Lipinski's rules, thus better supporting its suitability as a candidate for an oral drug.

Rutin has a relatively high molecular weight (approximately 610 Da), more than 10 hydrogen-bond acceptors, and more than 5 hydrogen-bond donors. These values exceed Lipinski's criteria, so rutin tends to have limitations in terms of membrane permeability and oral bioavailability. Nevertheless, rutin continues to exhibit strong biological activity as an enzyme inhibitor (α-glucosidase and α-amylase) due to multipoint interactions with catalytic residues. This means that, although rutin may not be optimal as a single oral drug, it remains a relevant bioactive candidate, particularly when formulated using drug delivery systems or used in combination with other compounds.

Lucidenic acid D1 has a molecular weight of approximately 500 Da, with the number of hydrogen bond acceptors and donors still within Lipinski's rules. This profile indicates that this compound adheres more closely to Lipinski's rules than rutin, suggesting it has the potential for better oral bioavailability. Furthermore, docking results show a very strong binding affinity (ΔG -9.8 kcal/mol) with key catalytic residues, supporting its role as an effective enzyme inhibitor.

Table 5. ADMET prediction results

Ligand	HIA	BBB	PPB (%)	Inhibition/ Substrate CYP	Carcinogenicity	Oral Toxicity Acute (kg/mol)
Cathecin	+	+	89,3 %	Inhibitor Substrate	Carcinogenic	0.271
Rutin	+	+	85.0%	Inhibitor Subtrate	Carcinogenic	0.044
Quercetin-3-o-glucoside	+	+	83.1%	Inhibitor Subtrate	Carcinogenic	0.053
Lucidenic acid D1	+	+	89.3%	Inhibitor Subtrate	Carcinogenic	0.243

Table 5 summarizes the pharmacokinetic and toxicological profiles of four bioactive compounds: catechin, rutin, quercetin-3-O-glucoside, and lucidenic acid D1. Each compound is analyzed based on its intestinal absorption capacity (HIA), permeability across the blood-brain barrier (BBB), plasma protein binding (PPB), interactions with cytochrome P450 (CYP) enzymes, carcinogenic potential, and acute oral toxicity values. All compounds showed positive results in the HIA and BBB assays, indicating that they are well absorbed in the intestine and have the potential to cross the blood-brain barrier. Plasma protein binding levels are quite high, ranging from 83-89%, suggesting that most of the compounds will be bound in the bloodstream, thereby affecting their distribution and bioavailability. All four compounds are also listed as CYP inhibitors/substrates, suggesting the possibility of interactions with the metabolism of other drugs. From a safety perspective, all compounds are classified as having carcinogenic potential, so special attention is required in further development. The average acute oral toxicity values indicate toxicity levels below 1. Lucidenic acid has a toxicity value of (0.243 kg/mol), followed by rutin, which exhibits a toxicity level of (0.044 kg/mol), while catechin (0.271 kg/mol) and lucidenic acid D1 (0.243 kg/mol) have higher values, indicating lower toxicity than rutin.

Flavonoid compounds (rutin, quercetin, catechin) show strong potential as α-glucosidase inhibitors, consistent with the literature that flavonoids can lower blood glucose by inhibiting carbohydrate breakdown. Flavonoids (e.g., quercetin), alkaloids, tannins, terpenoids, and catechins can inhibit carbohydrate digestive enzymes, thereby slowing glucose formation and lowering postprandial blood glucose levels. Procyanidin B has also been shown to increase glucose uptake by cells, mimicking the mechanism of insulin in maintaining glucose balance [20], [46], [3], [47]. Large polyphenolic compounds (rutin, procyanidin, lucidenic acid) have strong bonds, potentially inhibiting the degradation of starch into glucose. This supports the antidiabetic effect through the mechanism of digestive enzyme inhibition [48]-[50].

This study highlights the unique utilization of the non-edible husk of *Durio oxleyanus* as a novel source of bioactive compounds with antidiabetic potential. Unlike most research that focuses on edible fruit parts, our approach demonstrates that plant by-products can serve as sustainable reservoirs of flavonoids and polyphenols. The identification of rutin, quercetin, catechin, procyanidin B, and lucidenic acid as strong α-glucosidase and α-amylase inhibitors underscores the originality of this work in expanding the pharmacological relevance of underutilized plant materials. In addition to its scientific contributions, this study also highlights the importance of utilizing inedible plant parts for drug discovery. The use of fruit peel waste not only supports the principles of sustainability and the circular economy but also opens up new opportunities for discovering bioactive molecules with diverse pharmacological activities. This strategy aligns with global efforts to integrate green chemistry and the more comprehensive use of natural resources, thereby maximizing biodiversity to support human health. In the short term, this research provides a scientific basis for developing functional extracts or nutraceutical prototypes derived from *Durio oxleyanus* husk. The findings can guide further in vitro and in vivo validation studies, offering immediate opportunities for academic collaboration, student training, and the advancement of computational drug discovery methods in natural product research.

On a broader scale, the results contribute to the global search for safer, plant-based antidiabetic agents. By demonstrating the potential of non-edible plant parts, this study supports sustainable resource utilization and waste reduction in agricultural systems. Long-term, the integration of such bioactive compounds into therapeutic pipelines could reduce reliance on synthetic drugs, lower treatment costs, and promote biodiversity-based drug discovery strategies worldwide. Despite promising in silico and phytochemical findings, this study is limited by the absence of comprehensive in vitro and in vivo validation to confirm biological activity in physiological systems. The extraction process was restricted to methanol-water solvents, which may not fully capture non-polar constituents. Additionally, variability in plant material due to geographical and seasonal factors could influence reproducibility. Future work should include standardized extraction protocols, bioassays, and clinical studies to strengthen translational relevance.

4. CONCLUSION

This study shows that hydroalcoholic extracts from the huks of *Durio oxleyanus* (Sukang Durian) from Sabah contain various bioactive compounds, particularly flavonoids, polyphenols, and organic acids, which have potential as antidiabetic and antioxidant agents. Molecular docking simulation results show that several compounds, particularly catechin, rutin, malvidin-3-O-glucoside, lucidenic acid D1, and quercetin-3-O-glucosidase, have strong binding affinity to the α-glucosidase (2QMJ) and α-amylase (1B2Y) enzymes. Stable interactions with polar, aromatic, and acidic residues at the enzyme's active site support the mechanism of inhibiting starch hydrolysis into glucose, thereby potentially lowering postprandial blood glucose levels. Overall, this study confirms that the non-edible part of *Durio oxleyanus* is a promising source of phytochemicals for development as a natural antidiabetic therapeutic candidate.

Future research should not be limited to in silico docking simulations but should also include in vitro and in vivo tests to validate the inhibitory activity of these compounds against α-glucosidase and α-amylase under physiological conditions. Research on the synergistic effects among these phytochemical compounds, as well as their potential combination with existing antidiabetic drugs, may open up new therapeutic strategies. In addition, structure-activity relationship (SAR) studies can be conducted to optimize molecular characteristics that enhance inhibitory potential. Investigating synergistic effects among these phytochemical compounds, as well as their potential combination with existing antidiabetic drugs, could open up new therapeutic strategies. Finally, broader research on the sustainable use of inedible plant parts could strengthen the role of biodiversity in drug discovery and contribute to environmentally friendly approaches in natural product pharmacology.

ACKNOWLEDGEMENTS

The author would like to express his deepest gratitude to the University of Malaysia Sabah, Institute of Tropical Biology and Conservation, for the support and facilities provided during this research. Thanks are also extended to the local community in Sabah who assisted in the sampling process of *Durio oxleyanus*. The author

appreciates the constructive feedback from colleagues and reviewers who have contributed to improving the quality of this manuscript..

AUTHOR CONTRIBUTIONS

Conceptualization, Q.H., M.S. and S.A.; Methodology, S.A. and M.S. ; Formal Analysis, Q.H. ; Writing –Original Draft Preparation, Q.H. and M.H. ; Writing –Review & Editing, A.I.I. and E.F. ; Visualization, N.H. ; Supervision, M.S.

INFORMED CONSENT STATEMENT

Not applicable. This study did not involve human participants, clinical data, or animal experimentation..

CONFLICTS OF INTEREST

The author declares no conflict of interest related to this study.

USE OF ARTIFICIAL INTELLIGENCE (AI)-ASSISTED TECHNOLOGY

During the preparation of this manuscript, AI-assisted technology was used to support language refinement, structural organization, and academic writing improvement. All generated content was carefully reviewed, revised, and validated by the author. The author takes full responsibility for the scientific accuracy, originality, and integrity of the final manuscript.

REFERENCES

[1] D. R. Owens *et al*., "IDF Diabetes Atlas: A worldwide review of studies utilizing retinal photography to screen for diabetic retinopathy from 2017 to 2024 inclusive," *Diabetes Res. Clin. Pract.*, vol. 226, Art. no. 112346, Aug. 2025, doi: 10.1016/j.diabres.2025.112346.

[2] F. R. Putri, C. A. Osunla, and R. A. Sen, "Bridging healthcare and technology: Management systems in radiology services," *J. Health Innov. Environ. Educ.*, vol. 2, no. 1, pp. 31–42, 2025, doi: 10.37251/jhiee.v2i1.1726.

[3] S. Kassymbekova, J. Pepania, and M. Al Balushi, "Using a multi omic approach to investigate a diet intervention in young adults at risk of disease," *Multidiscip. J. Tour. Hosp. Sport Phys. Educ.*, vol. 2, no. 1, pp. 19–26, 2025, doi: 10.37251/jthpe.v2i1.1782.

[4] K. K. Pal, R. K. Rai, P. K. Tiwari, and A. K. Misra, "Role of awareness programs on diabetes prevention and control of viral infection: A study of optimal control," *Eur. Phys. J. Plus*, vol. 140, no. 2, Mar. 2025, doi: 10.1140/epjp/s13360-025-06063-z.

[5] H. K. Tran *et al*., "Extraction of flavonoids from durian (*Durio zibethinus*) fruit rinds and evaluation of their antioxidant, antidiabetic and anticancer properties," *Int. J. Food Sci. Technol.*, vol. 59, no. 3, pp. 1409–1420, Mar. 2024, doi: 10.1111/ijfs.16886.

[6] A. Tengah, W. F. W. Yusoff, H. Sajali, T. Sookkumnerd, and H. X. Vinh, "Mobile technology enhanced diabetes self-management education improves self-efficacy and glycaemic control in adults with type 2 diabetes," *J. Health Innov. Environ. Educ.*, vol. 2, no. 2, pp. 176–185, 2025, doi: 10.37251/jhiee.v2i2.2597.

[7] T. N. Mgwenya, H. Abrahamse, and N. N. Houreld, "Photobiomodulation studies on diabetic wound healing: An insight into the inflammatory pathway in diabetic wound healing," *Wound Repair Regen.*, vol. 33, no. 1, Art. no. e13239, 2025, doi: 10.1111/wrr.13239.

[8] X. Meng, H. Zhang, Z. Zhao, *et al*., "Type 3 diabetes and metabolic reprogramming of brain neurons: Causes and therapeutic strategies," *Mol. Med.*, vol. 31, Art. no. 61, 2025, doi: 10.1186/s10020-025-01101-z.

[9] M. M. Jackson and A. A. O. Alfaki, "Advancing Sustainable Development Goal 6: Innovations, challenges, and pathways for clean water and sanitation," *Indones. Sci. Educ. J.*, vol. 6, no. 3, pp. 224–231, Sep. 2025, doi: 10.37251/isej.v6i3.2114.

[10] C. Iancu *et al*., "The evaluation of normo-glycemic and cyto-regenerative effects of *Pelargonium* species extracts," *Farmacia*, vol. 68, no. 1, pp. 135–141, 2020, doi: 10.31925/farmacia.2020.1.19.

[11] J. Gangoiti, S. F. Corwin, L. M. Lamothe, C. Vafiadi, B. R. Hamaker, and L. Dijkhuizen, "Synthesis of novel α-glucans with potential health benefits through controlled glucose release in the human gastrointestinal tract," *Crit. Rev. Food Sci. Nutr.*, vol. 60, no. 1, pp. 123–146, 2020, doi: 10.1080/10408398.2018.1516621.

[12] M. Ijaz and S. H. Tandyo, "Roselle (*Hibiscus sabdariffa*) as a sustainable herbal supplement for enhancing the performance of freshwater ornamental fish," *J. Acad. Biol. Educ.*, vol. 2, no. 2, pp. 157–164, Dec. 2025, doi: 10.37251/jouabe.v2i2.2243.

[13] Q. Wang *et al*., "The antioxidant activities, inhibitory effects, kinetics, and mechanisms of artocarpin and α-mangostin on α-glucosidase and α-amylase," *Int. J. Biol. Macromol.*, vol. 213, pp. 880–891, Jul. 2022, doi: 10.1016/j.ijbiomac.2022.06.017.

[14] A. Sehrawat, J. Bhatti, I. Sidhu, J. Mishra, U. Navik, N. Khullar, *et al*., "Oxidative stress in the pathophysiology of type 2 diabetes and related complications: Current therapeutics strategies and future perspectives," *Free Radic. Biol. Med.*, vol. 184, pp. 114–134, 2022, doi: 10.1016/j.freeradbiomed.2022.03.019.

[15] F. Cabré, J. J. Centelles, and M. Cascante, "From current therapeutics to multitarget ligands: A review of diabetes pharmacological treatments," *Pharmaceutics*, vol. 17, no. 9, Art. no. 1125, 2025, doi: 10.3390/pharmaceutics17091125.

[16] S. Padhi, A. K. Nayak, and A. Behera, "Type II diabetes mellitus: A review on recent drug based therapeutics," *Biomed. Pharmacother.*, vol. 131, Art. no. 110708, Nov. 2020, doi: 10.1016/j.biopha.2020.110708.

[17] W. Xiao, W. Jiang, Z. Chen, *et al*., "Advance in peptide-based drug development: Delivery platforms, therapeutics and vaccines," *Signal Transduct. Target. Ther.*, vol. 10, Art. no. 74, 2025, doi: 10.1038/s41392-024-02107-5.

[18] X. Lu, Q. Xie, X. Pan, *et al*., "Type 2 diabetes mellitus in adults: Pathogenesis, prevention and therapy," *Signal Transduct. Target. Ther.*, vol. 9, Art. no. 262, 2024, doi: 10.1038/s41392-024-01951-9.
[19] C. C. Kuo, K. Moon, K. A. Thayer, and A. Navas-Acien, "Environmental chemicals and type 2 diabetes: An updated systematic review of the epidemiologic evidence," *Curr. Diab. Rep.*, vol. 13, no. 6, pp. 831–849, Dec. 2013, doi: 10.1007/s11892-013-0432-6.
[20] D. K. Patel, R. Kumar, D. Laloo, and S. Hemalatha, "Diabetes mellitus: An overview on its pharmacological aspects and reported medicinal plants having antidiabetic activity," *Asian Pac. J. Trop. Biomed.*, vol. 2, no. 5, pp. 411–420, 2012, doi: 10.1016/S2221-1691(12)60067-7.
[21] A. Kanwal, N. Kanwar, S. Bharati, P. Srivastava, S. P. Singh, and S. Amar, "Exploring new drug targets for type 2 diabetes: Success, challenges and opportunities," *Biomedicines*, vol. 10, no. 2, Art. no. 331, 2022, doi: 10.3390/biomedicines10020331.
[22] C. Sun *et al*., "Anti-diabetic effects of natural antioxidants from fruits," *Trends Food Sci. Technol.*, vol. 117, pp. 3–18, 2021, doi: 10.1016/j.tifs.2020.07.024.
[23] J. O. Unuofin and S. L. Lebelo, "Antioxidant effects and mechanisms of medicinal plants and their bioactive compounds for the prevention and treatment of type 2 diabetes: An updated review," *Oxid. Med. Cell. Longev.*, vol. 2020, Art. no. 1356893, 2020, doi: 10.1155/2020/1356893.
[24] L. Barrea, C. Vetrani, L. Verde, *et al*., "Comprehensive approach to medical nutrition therapy in patients with type 2 diabetes mellitus: From diet to bioactive compounds," *Antioxidants*, vol. 12, no. 4, Art. no. 904, 2023, doi: 10.3390/antiox12040904.
[25] Muhtadi, A. U. Primarianti, and T. A. Sujono, "Antidiabetic activity of durian (*Durio zibethinus* Murr.) and rambutan (*Nephelium lappaceum* L.) fruit peels in alloxan diabetic rats," *Procedia Food Sci.*, vol. 3, pp. 255–261, 2015, doi: 10.1016/j.profoo.2015.01.028.
[26] N. Charoenphun and W. K. Klangbud, "Antioxidant and anti-inflammatory activities of durian (*Durio zibethinus* Murr.) pulp, seed and peel flour," *PeerJ*, vol. 10, Art. no. e12933, 2022, doi: 10.7717/peerj.12933.
[27] Muhtadi, H. H., M. Rabbaniyyah, and A. Suhendi, "Pharmacological properties and toxicological investigation on *Durio zibethinus* Murr. peel extracts," *KnE Soc. Sci.*, vol. 8, no. 4, 2023, doi: 10.18502/kss.v8i4.12977.
[28] B. Kunarto and E. Y. Sani, "Antioxidant activity of extract from ultrasonic-assisted extraction of durian peels," *J. Appl. Food Technol.*, vol. 5, no. 2, 2018, doi: 10.17728/jaft.3309.
[29] N. Juarah, N. Surugau, N. A. Rusdi, M. F. Abu-Bakar, and M. Suleiman, "Phytochemical content and antioxidant properties of Bornean wild durian from Sabah," in *IOP Conf. Ser. Earth Environ. Sci.*, vol. 736, no. 1, Art. no. 012030, May 2021, doi: 10.1088/1755-1315/736/1/012030.
[30] S. Dallakyan and A. J. Olson, "Small molecule library screening by docking with PyRx," in *Chemical Biology: Methods and Protocols*, New York, NY, USA: Humana Press, 2015, pp. 243–250.
[31] G. Khaksar, S. Kasemcholathan, and S. Sirikantaramas, "Durian (*Durio zibethinus* L.): Nutritional composition, pharmacological implications, value-added products, and omics-based investigations," *Horticulturae*, vol. 10, no. 4, Art. no. 342, 2024, doi: 10.3390/horticulturae10040342.
[32] J. Feng, X. Yi, W. Huang, Y. Wang, and X. He, "Novel triterpenoids and glycosides from durian exert pronounced anti-inflammatory activities," *Food Chem.*, vol. 241, pp. 215–221, Feb. 2018, doi: 10.1016/j.foodchem.2017.08.097.
[33] J. Feng, Y. Wang, X. Yi, W. Yang, and X. He, "Phenolics from durian exert pronounced NO inhibitory and antioxidant activities," *J. Agric. Food Chem.*, vol. 64, no. 21, pp. 4273–4279, Jun. 2016, doi: 10.1021/acs.jafc.6b01580.
[34] S. Hokputsa, N. Gerddit, S. Pongsamart, K. Inngjerdingen, T. Heinze, B. S. Koschella, *et al*., "Water-soluble polysaccharides with pharmaceutical importance from Durian rinds (*Durio zibethinus* Murr.): Isolation, fractionation, characterisation and bioactivity," *Carbohydr. Polym.*, vol. 56, no. 4, pp. 471–481, Jul. 2004, doi: 10.1016/j.carbpol.2004.03.018.
[35] M. Masturi, A. Marwoto, Sulhadi, A. B. Cahyono, and S. Alighiri, "Identification of flavonoid compounds and total flavonoid content from biowaste of local durian shell (*Durio zibethinus*)," in *J. Phys.: Conf. Ser.*, vol. 1567, Jul. 2020, Art. no. 042084, doi: 10.1088/1742-6596/1567/4/042084.
[36] N. Sangkhonkhet, N. Phanchindawan, S. Lerdsuwan, W. Nalinanon, and D. Pisuttharachai, "Effect of *Durio zibethinus* Murr. cv. Monthong rind as a dietary ingredient in feed on the growth performance and disease resistance against *Aeromonas hydrophila* in red tilapia (*Oreochromis niloticus* × *Oreochromis mossambicus*)," *ASEAN J. Sci. Technol. Rep.*, vol. 26, no. 2, pp. 39–48, Apr. 2023, doi: 10.55164/ajstr.v26i2.248572.
[37] J. W. Pitera, "Expected distributions of root-mean-square positional deviations in proteins," *J. Phys. Chem. B*, vol. 118, no. 24, pp. 6526–6530, Jun. 2014, doi: 10.1021/jp412776d.
[38] D. Zhang, H. Li, H. Wang, and L. Li, "Docking accuracy enhanced by QM-derived protein charges," *Mol. Phys.*, vol. 114, no. 20, pp. 3015–3025, Oct. 2016, doi: 10.1080/00268976.2016.1213908.
[39] F. Ranjbary, F. Fathi, P. S. Pakchin, and S. Maleki, "Astaxanthin binding affinity to DNA: Studied by fluorescence, surface plasmon resonance and molecular docking methods," *J. Fluoresc.*, vol. 34, no. 2, pp. 755–764, Mar. 2024, doi: 10.1007/s10895-023-03310-3.
[40] I. Khosravi, M. Sahihi, H. A. Rudbari, G. Borhan, and Z. Chavoshpour-Natanzi, "The interaction of a new Schiff base ligand with human serum albumin: Molecular docking and molecular dynamics simulation studies," *J. Macromol. Sci. B*, vol. 56, no. 9, pp. 636–643, Sep. 2017, doi: 10.1080/00222348.2017.1356634.
[41] S. S. Elhady, M. A. Al-Huqail, M. S. Alwahibi, A. M. El-Garawani, A. A. M. Abdelgawad, M. M. Elshaer, *et al*., "Deciphering molecular aspects of potential α-glucosidase inhibitors within *Aspergillus terreus*: A computational odyssey of molecular docking-coupled dynamics simulations and pharmacokinetic profiling," *Metabolites*, vol. 13, no. 8, Art. no. 942, Aug. 2023, doi: 10.3390/metabo13080942.
[42] J. Januarto, "In silico analysis of the interaction between stevia compounds and the MGAM receptor as potential antidiabetic agents," *Indones. J. Pharm. Educ.*, vol. 5, no. 2, pp. 181–190, Apr. 2025, doi: 10.37311/ijpe.v5i2.31057.

[43] E. AlRashidi, S. Ghannay, A. E. A. E. Albadri, M. Abid, A. Kadri, and K. Aouadi, "Design, synthesis, biological evaluation, kinetic studies and molecular modeling of imidazo-isoxazole derivatives targeting both α-amylase and α-glucosidase inhibitors," *Heliyon*, vol. 10, no. 20, Art. no. e38376, Oct. 2024, doi: 10.1016/j.heliyon.2024.e38376.

[44] S. Fettach, N. El Brahmi, A. A. A. El Mzibri, H. A. Bouraada, M. Ramli, A. Ansar, *et al*., "Synthesis, α-glucosidase and α-amylase inhibitory activities, acute toxicity and molecular docking studies of thiazolidine-2,4-diones derivatives," *J. Biomol. Struct. Dyn.*, vol. 40, no. 18, pp. 8340–8351, 2022, doi: 10.1080/07391102.2021.1911854.

[45] M. Alp, A. Misturini, G. Sastre, and M. Gálvez-Llompart, "Drug screening of α-amylase inhibitors as candidates for treating diabetes," *J. Cell. Mol. Med.*, vol. 27, no. 15, pp. 2249–2260, Aug. 2023, doi: 10.1111/jcmm.17831.

[46] M. Rabbaniyyah and A. Suciati, "Anti-diabetes activity and phytochemical analysis of durian fruit methanol fraction," *Int. J. Islam. Complement. Med.*, vol. 4, no. 1, pp. 37–44, May 2023, doi: 10.55116/ijicm.v4i1.59.

[47] W. M. H. W. Zain, A. Mediani, N. K. Z. Zolkeflee, P. L. Wong, and F. Abas, "Antioxidant and alpha-glucosidase inhibitory activity of *Durio zibethinus* L. Clone 175 (Durian Udang Merah) shell and UHPLC-Orbitrap-MS profiling of the extract," *Sains Malays.*, vol. 53, no. 6, pp. 1281–1293, Jun. 2024, doi: 10.17576/jsm-2024-5306-05.

[48] N. T. H. Nguyen, T. T. T. Nguyen, D. T. C. Nguyen, and T. Van Tran, "A comprehensive review on the production of durian fruit waste-derived bioadsorbents for water treatment," *Chemosphere*, vol. 367, Art. no. 142801, Sep. 2024, doi: 10.1016/j.chemosphere.2024.142801.

[49] L. H. Ho and R. Bhat, "Exploring the potential nutraceutical values of durian (*Durio zibethinus* L.)—An exotic tropical fruit," *Food Chem.*, vol. 168, pp. 80–89, Feb. 2015, doi: 10.1016/j.foodchem.2014.07.020.

[50] N. S. Noorhashim, S. N. Azar, A. Azlan, N. A. Razali, A. R. Li, and N. H. K. Z. Abidin, "Total phenolic contents, total flavonoid contents and antioxidant activities of endocarp and mesocarp of Malaysian local *Durio zibethinus* (Musang King and Durian Kampung Peel)," *J. Food Meas. Charact.*, 2025, doi: 10.1007/s11694-025-03417-0.